Human Molecular Genetics, 2008, Vol. 17, No. 15 **2379–2389**
doi:10.1093/hmg/ddn138
Advance Access published on May 29, 2008

Novel variants in human Aquaporin-4 reduce cellular water permeability

Marco D. Sorani[1,2,†], Zsolt Zador[3,†], Evan Hurowitz[2], Donghong Yan[3], Kathleen M. Giacomini[2] and Geoffrey T. Manley[3,*]

[1]Program in Biological and Medical Informatics, [2]Department of Biopharmaceutical Sciences and [3]Department of Neurological Surgery, University of California, San Francisco, San Francisco, CA 94110, USA

Received January 13, 2008; Revised April 11, 2008; Accepted April 28, 2008

Cerebral edema contributes significantly to morbidity and mortality after brain injury and stroke. Aquaporin-4 (AQP4), a water channel expressed in astrocytes, plays a key role in brain water homeostasis. Genetic variants in other aquaporin family members have been associated with disease phenotypes. However, in human *AQP4*, only one non-synonymous single-nucleotide polymorphism (nsSNP) has been reported, with no characterization of protein function or disease phenotype. We analyzed DNA from an ethnically diverse cohort of 188 individuals to identify novel *AQP4* variants. *AQP4* variants were constructed by site-directed mutagenesis and expressed in cells. Water permeability assays in the cells were used to measure protein function. We identified 24 variants in *AQP4* including four novel nsSNPs (I128T, D184E, I205L and M224T). We did not observe the previously documented M278T in our sample. The nsSNPs found were rare (∼1–2% allele frequency) and heterozygous. Computational analysis predicted reduced function mutations. Protein expression and membrane localization were similar for reference AQP4 and the five AQP4 mutants. Cellular assays confirmed that four variant AQP4 channels reduced normalized water permeability to between 26 and 48% of the reference ($P < 0.001$), while the M278T mutation increased normalized water permeability ($P < 0.001$). We identified multiple novel *AQP4* SNPs and showed that four nsSNPs reduced water permeability. The previously reported M278T mutation resulted in gain of function. Our experiments provide insight into the function of the AQP4 protein. These nsSNPs may have clinical implications for patients with cerebral edema and related disorders.

INTRODUCTION

Cerebral edema, the abnormal accumulation of water in the brain parenchyma, can be a significant consequence of injury from brain trauma and stroke. Each year, approximately 1.4 million people in the USA alone suffer from traumatic brain injuries (TBI) (http://www.cdc.gov/ncipc/tbi/TBI.htm), and another 750 000 people suffer from strokes (http://www.stroke.org). Cerebral edema is a common pathophysiology after these events and can lead to elevated intracranial pressure, brain herniation and death. Phenotypic analysis of Aquaporin-4 (*AQP4*, OMIM *600308, NM_001650.4) knockout mice has provided evidence for the involvement of AQP4 in cerebral water balance (1). AQP4-null mice exhibit reduced brain swelling and improved neurological outcome in models of cytotoxic cerebral edema. However, in humans, only one naturally occurring non-synonymous single-nucleotide polymorphism (nsSNP) (rs3906956, M278T) has previously been reported in *AQP4*, with no functional characterization.

Aquaporin-4 is a member of a family of bidirectional, high-capacity water channels. AQP4 is primarily expressed in the foot processes of astrocytes throughout the central nervous system, particularly at the blood-brain and brain-cerebrospinal fluid barriers, and it is critical for brain water homeostasis. Characteristics of the *AQP4* gene and protein have been extensively described. The human *AQP4* gene (18q11.2–q12.1) is highly conserved, demonstrating over 90% sequence identity with mouse and rat orthologs. It is composed of five exons encoding 22, 127, 55, 27 and 92 amino acids and separated by introns of 2.7, 0.8, 0.3 and 5.2 kb (Fig. 1A). The 34 kDa

*To whom correspondence should be addressed at: Department of Neurosurgery, University of California, San Francisco, 1001 Potrero Ave., Room 101, San Francisco, CA 94110, USA. Tel: +1 4152064536; Fax: +1 4152063948; Email: manleyg@neurosurg.ucsf.edu
†The authors wish it to be known that, in their opinion, the first two authors should be regarded as joint First Authors.

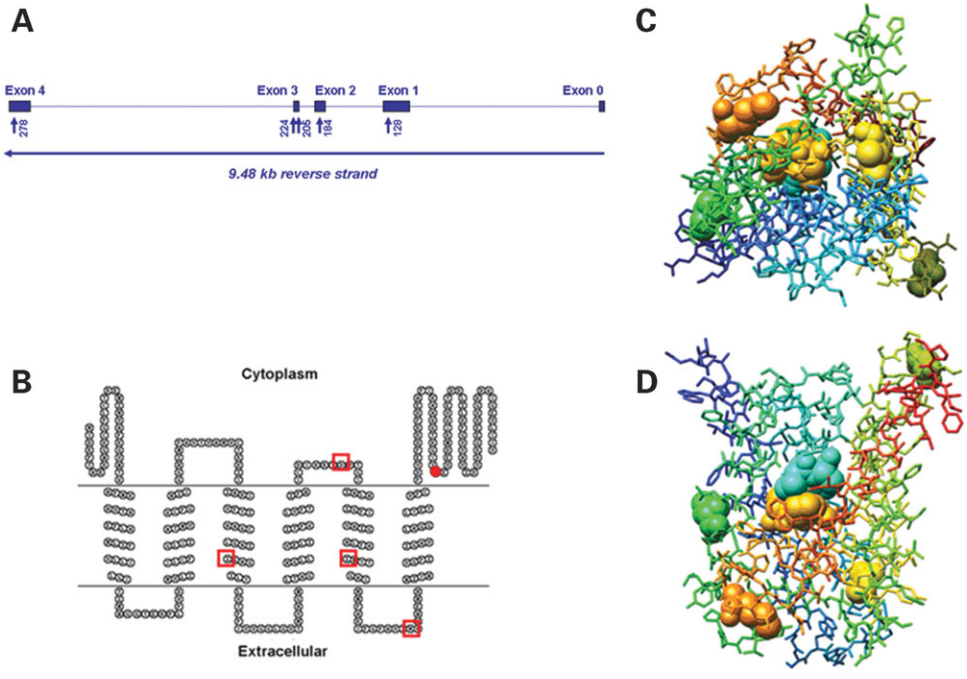

Figure 1. (**A**) Characteristics of the AQP4 gene. The long isoform of AQP4 is composed of five exons. The 323 amino acid protein includes six transmembrane domains, and its central structure consists of the large Major Intrinsic Protein domain. (**B**) Schematic secondary structure of AQP4, showing the intra-cellular N-and C-terminal domains, the six transmembrane domains and five loops, the four novel SNPs (squares), and the previously identified M278T (circle). Figure generated by TOPO2 (http://www.sacs.ucsf.edu/TOPO-run/wtopo.pl). (**C** and **D**) Three-dimensional crystal structure of rat AQP4 (PDB code, 2d57) with 93% identity to human AQP4, showing the four novel nsSNPs (green, orange, yellow, yellow-green) we identified distal to the pore motifs (yellow and blue), (C) looking through the channel and (D) profile view. Figures generated by UCSF Chimera (http://www.cgl.ucsf.edu/chimera).

AQP4 protein belongs to the Major Intrinsic Protein superfamily, and its central structure consists of a large domain of that same name. Because of several solved aquaporin crystal structures including rat AQP4 (2), many structural features of the aquaporin family are well documented, including the six alpha-helical transmembrane domains (Fig. 1B) that partially surround two shorter helices, the two Asn-Pro-Ala (NPA) motifs that form the pore (3), and the tetramers formed by AQP4 monomers (4).

Previous cellular studies using site-directed mutagenesis to introduce synthetic mutations (5–7) and naturally occurring (8,9) protein-altering nsSNPs in a variety of human aquaporins have shown that some variants can disrupt water permeability. For example, permeability measurements for the naturally occurring AQP2 variants associated with nephrogenic diabetes insipidus, R254L (10) and L22V (11) showed partial loss of function (28 and 69% of reference, respectively). Such data are significant because they show that even aquaporin variants with incomplete reduction of water permeability can be disease-associated. Synthetic variants have also been constructed to probe protein function. In *AQP4*, variants were created to test why the protein is insensitive to the mercurial inhibitor, $HgCl_2$ (12). An A188C mutation did not make AQP4 mercurial-sensitive, whereas point mutations at other residues proximal to the NPA motifs did impart mercurial-sensitivity, suggesting that those residues were near the aqueous pathway.

In this study, we sequenced *AQP4* in an ethnically diverse cohort of 188 subjects and identified 24 variants including four novel non-synonymous SNPs and three novel synonymous SNPs. We then performed computational prediction of the functional effects of these variants and tested our predictions by using a cell-based water permeability assay. We describe four reduced function nsSNPs and, interestingly, one gain-of-function nsSNP, all with implications for better understanding AQP4 function and for differential human response to cerebral edema and other disorders of water homeostasis.

RESULTS

Identification of nsSNPs

From our sequencing effort of the five *AQP4* exons, including short flanking sequences, we identified 24 variable sites. These variants included seven previously unknown coding SNPs, of which four were non-synonymous and three were synonymous (Table 1). In addition to the previously documented M278T SNP, not found in our sample, the four nsSNPs we found were I128T, D184E, I205L and M224T. The other two synonymous SNPs we found were the previously identified P67 and L164. The other 15 sites were in intronic or untranslated regions of the gene and included six previously unknown SNPs. The four nsSNPs we found were rare (~1–2% allele frequency overall and in affected ethnic groups) and heterozygous.

The four novel nsSNPs were each found in either two or three individuals of two different races or ethnicities.

Table 1. Summary of variants in AQP4, from 3′ to 5′ on the negative strand. Identification numbers are dbSNP rs numbers or our own IDs.

	Gene region	ID	Genomic position	Nucleotide change	Amino acid position	Amino acid change	AA frequency	CA frequency	AS frequency	ME frequency
1	3′-UTR	rs3763043[a]	22 689 816	G>A			0.239	0.317	0.415	0.468
2	3′-UTR	3151	22 689 869	G>C			0.022	0	0	**0.011**
3	3′-UTR	3150	22 689 890	C>T			0.196	0	0	0
4	3′-UTR	rs9807747	22 689 928	T>C			0.043	0	0	0
5	3′-UTR	3148	22 689 953	A>C			0	0.024	0	0
6	Coding	3147	22 690 326	A>G	273	Thr=Thr	**0.011**	0	0	0
7	Non-coding	3146	22 690 502	T>A			**0.011**	0	0	0
8	Non-coding	3145	22 690 517	T>C			0.106	0.224	0.424	0.381
9	Coding	3144	22 694 737	T>C	230	His=His	0	**0.011**	0	0
10	Coding	3143	22 694 756	T>C	224	Met>Thr	0	**0.011**	0	**0.011**
11	Coding	3142	22 694 814	A>C	205	Ile>Leu	**0.011**	0	0	0.021
12	Non-coding	3141	22 694 882	G>A			0.074	0	0	0
13	Coding	3140	22 695 153	T>A	184	Asp>Glu	0.021	0	0	**0.011**
14	Coding	rs1839318[a]	22 695 213	G>A	164	Leu=Leu	0.043	0.06	0	0.023
15	Non-coding	rs455671	22 696 054	T>C			0.043	0.189	0.383	0.151
16	Non-coding	3221	22 696 105	T>C			**0.011**	0	0	**0.012**
17	Non-coding	3220	22 696 128	A>G			0.021	0	0	0
18	Coding	3219	22 696 208	T>C	128	Ile>Thr	**0.011**	0	0	**0.012**
19	Coding	3218	22 696 225	G>A	122	Gln=Gln	0.021	0.054	0	**0.012**
20	Coding	rs35248760	22 696 390	G>T	67	Pro=Pro	0.021	0.149	0	0.035
21	Non-coding	3216	22 696 578	T>C			**0.011**	0	0	0
22	5′-UTR	rs162008	22 699 690	G>A			0.074	0.183	0.372	0.16
23	5′-UTR	3130	22 699 693	T>C			0.021	0	0	0
24	Promoter	rs162007	22 699 845	C>T			0.074	0.183	0.372	0.17

Allele frequency values in bold indicate singletons by ethnicity (AA, African American; CA, Caucasian American; AS, Asian American; ME, Mexican American; Asian Americans are of Chinese ancestry). Up to 47 individuals (94 chromosomes) were examined in each ethnic group.
[a]Found in HapMap.

Specifically, I128T, D184E and I205L were found in African Americans and Mexican Americans, while M224T was found in Mexican Americans and Caucasians. We found no coding nsSNPs in Chinese Americans. Of the total set of 24 variants, 21 were found in African Americans (including six singletons), 14 were found in Mexican Americans (including six singletons), 10 were found in Caucasian Americans (including two singletons) and five were found in Chinese Americans (no singletons). All singletons were verified.

Of the previously identified SNPs, two (rs1839318, a synonymous coding SNP, and rs3763043, in the 3′-UTR) were found in the HapMap cohort. We compared allele frequencies in our Caucasian, African American and Chinese American groups with the CEU (Utah residents of European ancestry), YRI (Yorubans in Nigeria) and CHB (Han Chinese in Beijing) groups from HapMap. We found concordance of frequencies for both variants across the three pairs of ethnic groups (rs3763043: 30.8 versus 32.5%, 23.9 versus 18.3%, 41.5 versus 30.0%; rs1839318: 3.9 versus 2.5%, 4.3 versus 3.3%, 0.0 versus 1.1%).

Assessment of haplotypes and linkage

We used the Haploview software to identify haplotypes, and we numbered them (*1, etc.) according to frequency and similarity (13). The frequencies of major haplotypes among ethnic groups reveal substructures in those populations (Fig. 2). The African American group has the most variants but also a single haplotype accounting for a large portion of the population sample (43.8% of samples in the major haplotype and 11.0% in the next most common haplotype). The Caucasian American group is similar, with 34.5% of the samples having the major haplotype and 17.9% in the next most common haplotype. On the other hand, the Chinese American and Mexican American groups both have two major haplotypes of nearly equal frequencies (38.8 and 32.8, 32.6 and 31.8%). The *1 haplotype is the primary haplotype in the African American, Caucasian American and Mexican American groups while *2 is the most common haplotype among Chinese Americans.

We next assessed linkage disequilibrium (LD) (Fig. 3) and reviewed D′ statistics (14). Among Chinese Americans, the few variants were all in LD. In the other three ethnicities, LD was less common, but four variant pairs had LOD scores greater than 2 and D′ greater than 0.7: rs162008 with rs162007, rs455671 with rs162007, rs455671 with rs162008 and rs3763043 with the novel pmt3145_T>C. We found few cases of LD with the four nsSNPs. In African Americans, the D184E SNP was in LD with the L164 SNP, and the I128T SNP was in LD with a novel, non-coding singleton. In Mexican Americans, the same linkage was seen for I128T.

We also assessed variation characteristics of the genomic region. Two of the previously identified variants (rs3763043, discussed above, and rs9807747, also in the 3′-UTR) and three novel variants (pmt3151_G>C, pmt3150_C>T, pmt3148_A>C) reside in a genomic region of higher heterozygosity ($\sim$0.25 kb^{-1}), or variant frequency, according to the HapMap browser. Two other previously identified variants (rs162008 and rs162007, both upstream) and one novel variant (pmt3130_T>C) reside in a genomic region of

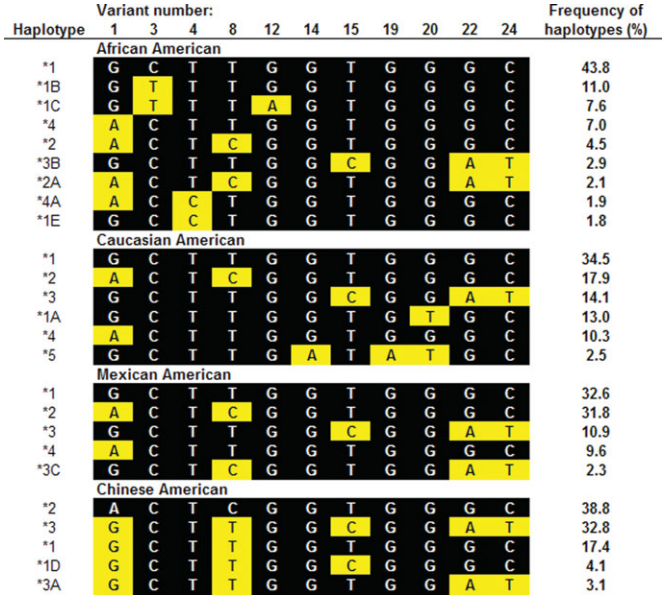

Haplotype	Variant number: 1	3	4	8	12	14	15	19	20	22	24	Frequency of haplotypes (%)
African American												
*1	G	C	T	T	G	G	T	G	G	G	C	43.8
*1B	G	T	T	T	G	G	T	G	G	G	C	11.0
*1C	G	T	T	T	A	G	T	G	G	G	C	7.6
*4	A	C	T	T	G	G	T	G	G	G	C	7.0
*2	A	C	T	C	G	G	T	G	G	G	C	4.5
*3B	G	C	T	T	G	G	C	G	G	A	T	2.9
*2A	A	C	T	C	G	G	T	G	G	A	T	2.1
*4A	A	C	C	T	G	G	T	G	G	G	C	1.9
*1E	G	C	C	T	G	G	T	G	G	G	C	1.8
Caucasian American												
*1	G	C	T	T	G	G	T	G	G	G	C	34.5
*2	A	C	T	C	G	G	T	G	G	G	C	17.9
*3	G	C	T	T	G	G	C	G	G	A	T	14.1
*1A	G	C	T	T	G	G	T	G	T	G	C	13.0
*4	A	C	T	T	G	G	T	G	G	G	C	10.3
*5	G	C	T	T	G	A	T	A	T	G	C	2.5
Mexican American												
*1	G	C	T	T	G	G	T	G	G	G	C	32.6
*2	A	C	T	C	G	G	T	G	G	G	C	31.8
*3	G	C	T	T	G	G	C	G	G	A	T	10.9
*4	A	C	T	T	G	G	T	G	G	G	C	9.6
*3C	G	C	T	C	G	G	T	G	G	A	T	2.3
Chinese American												
*2	A	C	T	C	G	G	T	G	G	G	C	38.8
*3	G	C	T	T	G	G	C	G	G	A	T	32.8
*1	G	C	T	T	G	G	T	G	G	G	C	17.4
*1D	G	C	T	T	G	G	C	G	G	G	C	4.1
*3A	G	C	T	T	G	G	T	G	G	A	T	3.1

Figure 2. Haplotypes are shown by allele frequency for each ethnic group. Frequencies reveal population substructure. The African American group is most homogenous, while the Chinese American and Mexican American groups both have two major haplotypes. Variant alleles are highlighted in yellow. Singletons are not shown.

higher recombination rate (5–10 cM/Mb). Recombination is an important biological determinant of LD. In regions of low recombination, few of the possible haplotypes will actually be observed in the population (15). Linkage information is more useful in association studies where a marker variant may be associated with a phenotype and linked to a causal variant. It is usually of little practical relevance when linkage is high but an allele is rare.

Computational prediction

Positional evolutionary conservation has been shown to be highly predictive of whether SNPs will be deleterious. We used three established methods as well as qualitative analysis to predict the effects of the five non-synonymous SNPs. The evolutionary matrices, PAM40 (16) and Blosum62 (17), indicated that every substitution except the Ile to Leu change at position 205 would be deleterious (Table 2). On the other hand, predictions of the SIFT (Sort Intolerant From Tolerant) algorithm (18) anticipated the greatest deleterious effect for I205L, with lesser effects for I128T and D184E. However, inspection of a multiple sequence alignment among mammalian orthologs plus chicken (Fig. 4) shows nearly perfect conservation at the mutated positions with just two conservative changes between human and chicken (I128V and M278I), suggesting that changes are selected against and could be deleterious. In fact, the chimp and human AQP4 proteins are identical except for a minor physicochemical V304I change.

Because of the highly conserved nature of *AQP4*, we next examined structural characteristics to predict the effects of the SNPs. Since all five occur far from the NPA motifs of the AQP4 channel pore, we would not necessarily expect complete ablation of function. MUpro (19) calculations indicated decreased protein stability for all five changes. Qualitatively, the Asp-Glu and Ile-Leu substitutions are minor chemical changes, while the Ile-Thr and Met-Thr substitutions result in more significant changes, from hydrophobic to hydrophilic residues with smaller volume. Furthermore, Ile-Thr eliminates an aliphatic residue while Met-Thr results in the loss of a sulfur atom. Of the five nsSNPs, I128T is in a transmembrane domain, D184E and I205L are at helix-loop boundaries, and M224T is in a loop. M278T is in the C-terminal domain, suggesting a possible role in sorting (Fig. 1C).

Expression and localization

We created stably transfected cells expressing reference and variant AQP4 for use in a water permeability assay (Fig. 5). As aquaporins are membrane proteins, their degree of expression and localization to the membrane would likely affect water permeability. We examined whether the five nsSNPs affected protein expression and localization. Cell surface proteins were biotinylated and isolated by streptavidin. By western blot with an AQP antibody, we confirmed AQP4 expression by detecting a $\sim$36 kDa band corresponding to the protein and faint accessory bands representing glycosylated AQP4, as has been observed by others (Fig. 5C, lanes 4–8) (20). We found that most of the protein for reference and mutant proteins localized to the plasma membrane. The total protein expression levels were comparable among reference and mutant proteins. Blots that were stripped and reprobed for the intracellular enzyme GAPDH showed no signal in the biotinylated samples, indicating specific membrane labeling, whereas the positive control of whole cell lysate demonstrated a $\sim$37 kDa band corresponding to GAPDH.

Water permeability measurements

We next assessed the effects of the nsSNPs on protein function by measuring water permeability using a cell swelling assay (21,22). The measurements resulted in swelling curves as shown in Fig. 5A, and the measurement procedure is represented in Fig. 5B. From the curves, we identified the $t_{1/2}$ by fitting the curve to a single exponential equation. Permeability was calculated based on $t_{1/2}$ as described previously (23). Cells transfected with reference and all mutant proteins swelled significantly faster than untransfected cells, as expected. Previous work has shown that AQP protein expression directly correlates with the overall water permeability of the cell membrane (24). To take this into account, we calculated relative water permeability by normalizing the permeability against values of cell surface AQP4 protein quantified by cell surface biotinylation. We found that the nsSNPs found in our cohort (I128T, D184E, I205L and M224T) had lower relative water permeability, reduced to $48.3 \pm 11.5\%$, $36.3 \pm 8.1\%$, $25.6 \pm 5.8\%$ and $31 \pm 5.6\%$ of reference AQP4, respectively ($P < 0.001$ for each) (Fig. 5D). Interestingly, the variant predicted by SIFT to be most deleterious, based on evolutionary conservation, was I205L which did in fact produce the greatest reduction in water permeability ($P < 0.001$). On the other hand, the previously reported M278T variant in the C-terminal domain

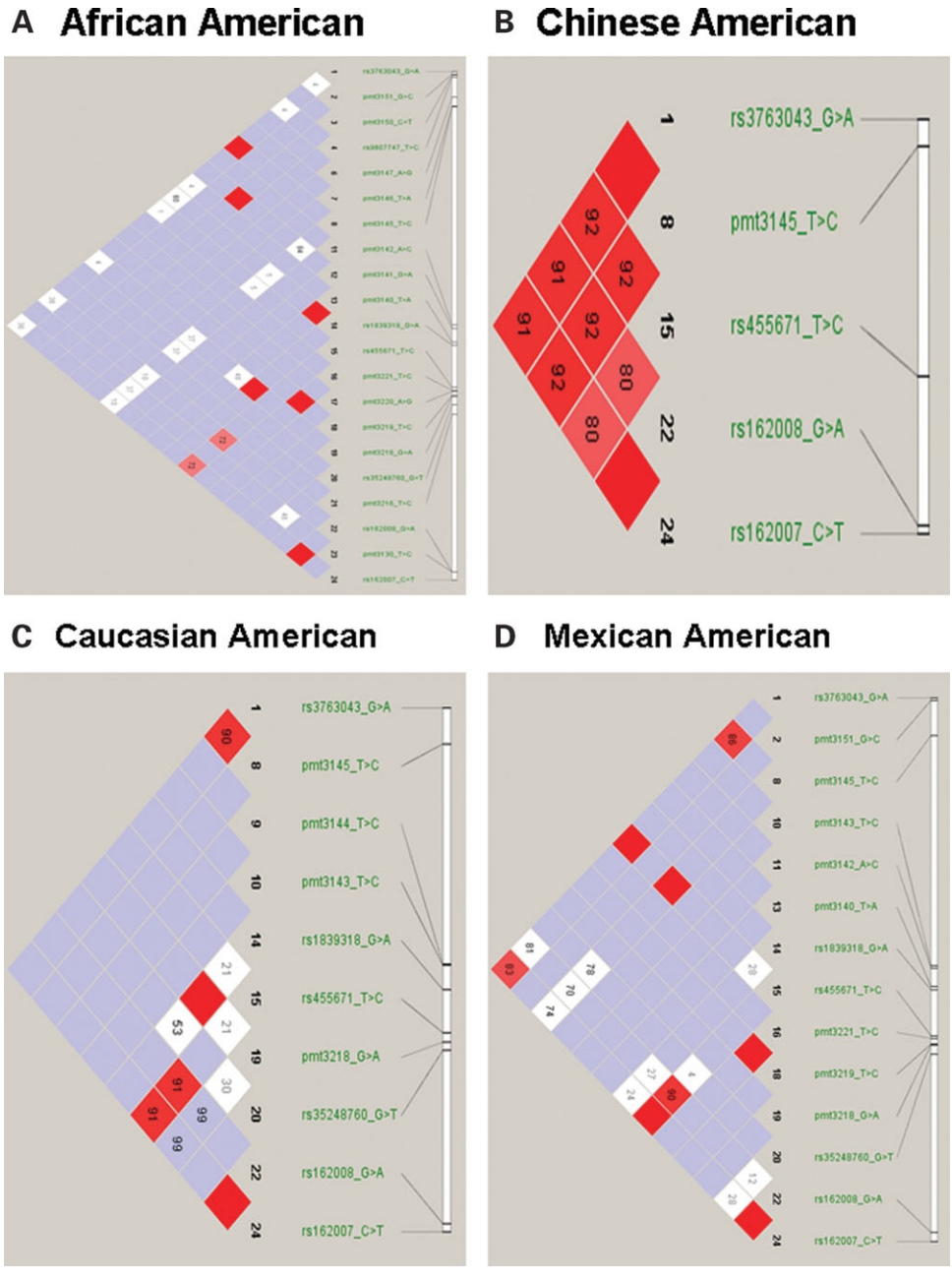

Figure 3. Linkage disequilibrium plots with variant IDs and position in the gene. D′ < 1 and LOD < 2 white, D′ < 1 and LOD ≥ 2 shades of pink/red, D′ = 1 and LOD ≥ 2 bright red. LD is high for the few variants in Chinese Americans but generally low in other ethnicities. There were few cases of LD among the four nsSNPs. In African Americans, the D184E SNP was in LD with the L164 SNP, and the I128T SNP was in LD with a novel, non-coding singleton. In Mexican Americans, the same linkage was seen for I128T.

showed similar expression and localization and increased relative water permeability (138.1 ± 9.0%, $P < 0.001$) (Fig. 6).

DISCUSSION

In an ethnically diverse sample set consisting of DNA from 188 individuals, we identified 24 variants in *AQP4* including four novel coding non-synonymous SNPs. We did not observe the one previously documented nsSNP in *AQP4*. While previous reports have indicated that non-coding variants in *AQP4* can have an impact on function (25–27), we did not fully sequence the non-coding regions. We focused on these five non-synonymous coding variants because we expected them to result in the most significant functional effects. Functional characterization of the SNPs revealed four with reduced function and one with a gain of function. All variants were evaluated using population analysis and computational effect prediction, and the nsSNPs were further characterized using an established experimental method to measure cell swelling and water permeability.

Table 2. Computational SNP effect predictions based on evolutionary conservation and protein stability from two servers and two substitution matrices

	SIFT	MUpro	Blosum62	PAM40
I128T	0.13	**−1.89**	**−1**	**−3**
D184E	0.19	**−1.02**	**−1**	**−2**
I205L	**0.05**	**−0.81**	2	3
M224T	0.64	**−1.81**	**−1**	**−3**
M278T	0.59	**−1.33**	**−1**	**−3**

SIFT scores less than or equal to 0.05, and MUpro as well as matrix scores less than zero suggest deleterious effect, in bold. Taken together, the scores suggest all variants have some functional effect.

Novel, rare variants identified

Compared with the 61 variants listed in dbSNP, the 17 new variants identified in this study after sequencing the exonic and flanking regions represent an increase of 28% in known *AQP4* variation. The gene is known to be well-conserved, and nsSNPs were rare (∼1–2% allele frequencies).

Haplotypes suggest population structure

The frequencies of the major haplotypes among ethnic groups reveal substructures in those populations. The *1 haplotype is the primary haplotype in the African American, Caucasian American and Mexican American groups while *2 is the most common haplotype among Chinese Americans. The large Wellcome Trust Consortium study showed that genomic regions can show strong geographical variation within the same ethnicity, in that case Caucasians (28). Our subjects were all from San Francisco, but variation due to admixture, heterogeneous immigration and other factors appears to exist.

Computational prediction indicates partial deleterious effects

Due to the time, cost and variability of experimental characterization, computational predictions can help provide insight and prioritize experiments, but at least four factors complicate the prediction of the effects of aquaporin SNPs. First, while water transport is the main function of AQP4, it has also recently been shown to be involved in cellular adhesion, potassium kinetics, signal transduction, cell migration, scar formation, glutamate uptake, regulation of connexin43 and reduction in cell coupling (29,30). Even the use of multiple assays could overlook changes in these or other unknown functions (31). Second, since aquaporins demonstrate high evolutionary conservation, most residue substitutions would not appear to be tolerated. SIFT predictions correctly identified I205L as the SNP with the greatest effect and also suggested that, given the low scores for I128T and D184E, these variants may result in partial reduction of permeability. Third, the low allele frequencies of all four nsSNPs suggest deleterious effects (31). Fourth, the MUpro calculations indicated that while none of the variants appear to directly alter the conformation or selectivity of the pore, all five decreased protein stability. This finding is consistent with previous reports that variants primarily act to destabilize structure (32).

Expression and localization of AQP4 mutants are normal

The results of western blot and cell-surface biotinylation experiments demonstrate consistent protein expression and membrane localization. These factors are critical to reliable measurement of AQP4 water permeability. Notably, while our cell-based system is mammalian and robust, a number of studies show AQP4 to be highly clustered around blood vessels, subpial membranes and perisynaptic areas *in vivo* (33). This arrangement is supported by members of the dystroglycan complex that enable attachment to the extracellular matrix. The cells in our *in vitro* system are not polarized, but we do not expect this to affect our ability to compare the relative function of AQP4 mutants versus the reference protein in the same system. Furthermore, we show that the mutant proteins localize to the membrane, unlike some other previously reported aquaporin mutants, suggesting that the mechanism of effect of the mutations is related to other factors.

Mutants reduce water permeability

The four reduced function mutations inhibited permeability by similar degrees, to between 26 and 48% of the reference channel. Because their effects are not more severe, they most likely do not directly disrupt the water channel pore. Numerous studies have shown that synthetic and natural mutations near the pore generally abolish permeability (34). Rather, the mutations we found may affect turnover or efficiency of targeting to the membrane. Previous studies of mutations that did not reside near the pore show similar results, as with R254L and L22V in AQP2. The precise mechanisms responsible for the reduction in water permeability by the *AQP4* SNPs remain to be defined.

The prediction that I205L would be most deleterious due to its high degree of evolutionary conservation was confirmed by our functional studies and is supported by previous findings in other aquaporins. By alignment, I205L resides next to the G175 and C181 positions in AQP2 whose mutations are deleterious. It is also near C189 in AQP1 which has previously been mutated to gain insight into the structure and function of the channel. C189 plays a role in mercurial-sensitivity, and mutations resulted in negligible water permeability (35).

Of the other SNPs, I128T and D184E also reside near functionally important sites. In a multiple alignment, I128T aligns next to G100, a mutation hot-spot in AQP2, as indicated by the association of G100Stop (36), G100V (37) and G100R (38) with nephrogenic diabetes insipidus. D184 resides near S180, a consensus site for protein kinase C phosphorylation. In a previous study, reduction of AQP4 water permeability by phorbol dibutyrate and dopamine was abolished by mutation of S180, indicating that permeability had been decreased via phosphorylation (39). The region around M224T has not, to our knowledge, been functionally characterized in aquaporins.

Figure 4. Multiple sequence alignment of AQP4 orthologs spanning identified SNPs (in grey) and showing high evolutionary conservation, suggesting selective pressure. ('*', identical; ':', conserved physicochemical substitutions; '.', semi-conserved substitutions.)

M278T is a gain-of-function mutation

In our population of 188 subjects, we did not observe any occurrences of the M278T variant reported by The SNP Consortium for which we measured gain of function. M278T may be a very rare or 'personal' SNP. The M278T gain-of-function mutation is of interest given that AQP4 is already a high-capacity channel that has been highly conserved and optimized. The result also serves as an internal control for our assay, indicating that the reduced function measured for the other variants is not an automatic result. There is precedent for gain-of-function variants in aquaporins. The AQP7 variant, R12C, shows 118% permeability compared with reference but was only found in one subject, so association with phenotype was not determined. A detrimental gain-of-function mutation in AQP0 is involved in cataract phenotypes in mice (40,41).

Given its location in a terminal domain, it is unlikely that the M278T SNP alters pore selectivity or efficiency, but it could be acting in several other ways to result in AQP4 gain of function, including altered sorting, recycling and complex assembly. Previous work has shown that in the C-terminal basolateral targeting motif GSYMEV, the serine is phosphorylated by casein kinase II, and the clathrin adaptor proteins AP2 and AP3 interact with the tyrosine and valine residues (42). The M278T mutation directly alters this motif. Another study showed that the residues between V276 and I280 play a role in the expression of AQP4 in the membrane (43). Other previous studies have shown that mutations that introduce a Thr can result in gain of function via phosphorylation (44,45).

Clinical implications

The *AQP4* SNPs we identified are potentially clinically relevant. Just as AQP4 knock-out mice experience less astrocytic swelling and improved survival after cytotoxic edema, even partial knock-down SNPs in humans could have similar protective effects. Epidemiological studies have identified ethnicity-based differences in outcome after brain injury that could be based on allelic differences in various genes. Given the estimated 1.4 million TBI and 750 000 strokes in the USA alone each year, not including edematous tumors and other disorders of water imbalance, the five novel nsSNPs with 1% frequency could affect outcomes in over 100 000 people.

AQP4 variants may affect phenotypes beyond cerebral edema as well. Previous studies have shown that AQP4 deficiency slows astrocyte migration in response to chemotactic stimulus *in vitro*, and AQP4 deletion impairs glial scar progression following injury *in vivo* (46). Variants in *AQP4* sequence and expression have recently also been associated with seizure (47) and epilepsy (48), Duchenne's muscular dystrophy (49), HIV dementia (50), lupus (51), neuromyelitis optica and multiple sclerosis (52), and Crohn's disease and infectious colitis (53). Furthermore, there is evidence that abnormal AQP4 levels are associated with degenerative diseases, as shown in a Parkinson's disease mouse model (54). AQP4 is also expressed in the kidney, airways, stomach and colon, so it may be involved in other phenotypes as well.

Sequencing only exonic regions, we found multiple novel variants, and all five coding variants we assayed had functional consequences. Since functional data on variants in aquaporins are incomplete, our work has implications for

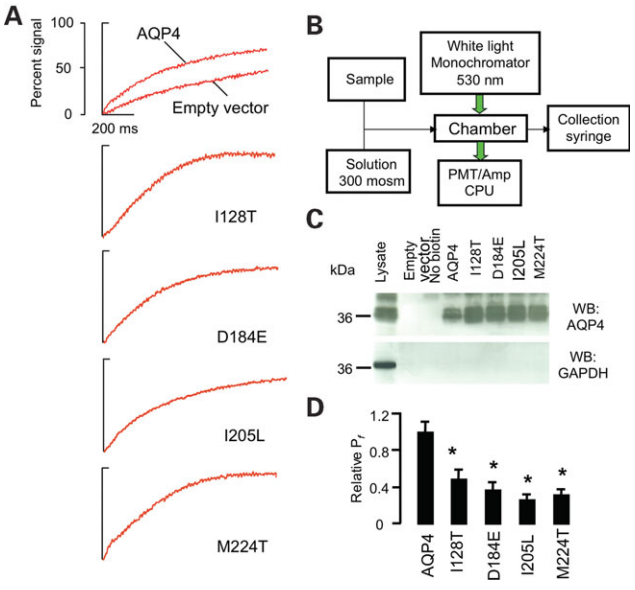

Figure 5. (**A**) Original light scattering curves of a single recording of CHO cell suspensions, expressing different AQP4 mutants. (**B**) Schematic of the light scattering experiments. (**C**) Cell-surface proteins were biotinylated, isolated by strepavidin and blotted with an AQP4 antibody. Western blots of biotinylated cell-surface protein demonstrating consistent membrane protein expression of AQP4 mutants (lanes 4–8). (**D**) Relative water permeability calculated from the individual $t_{1/2}$ normalized to the cell surface AQP4 expression. I128T, D184E, I205L and M224T had lower water permeability relative to reference, reduced to 48.3 ± 11.5%, 36.3 ± 8.1%, 25.6 ± 5.8% and 31 ± 5.6%, respectively ($P < 0.001$).

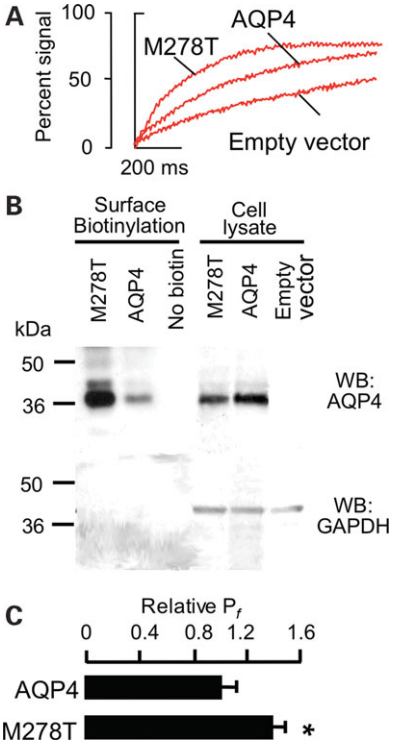

Figure 6. For the M278T SNP not found in our sample set, (**A**) representative light scattering curve for the CHO cell suspensions transfected with the empty vector, AQP4 and the M278T variant. (**B**) Western blots quantifying surface protein expression of AQP4 M278T. (**C**) Relative water permeability calculated from the individual $t_{1/2}$ and normalized cell surface AQP4 expression. The M278T variant showed increased relative water permeability (138.1 ± 9.0%, $P < 0.001$).

other genes in the family and their phenotypes. Deeper sequencing, especially in ethnically diverse populations, will identify new variants that may play a role in human health. Characterization of the effects of these and other still- unidentified aquaporin variants could lead to better understanding of the function of these important proteins and their clinical implications.

MATERIALS AND METHODS

Subjects

In previous work, we collected DNA samples from a large, self-identified, ethnically diverse cohort of healthy volunteers from the San Francisco Bay Area called SOPHIE (Studies of Pharmacogenetics in Ethnically Diverse Populations) (55). In this study, we screened for variants in *AQP4* in 188 subjects, including 47 African Americans, 47 Caucasian Americans, 47 Chinese Americans and 47 Mexican Americans from SOPHIE. Genomic and cDNA sequences of *AQP4* were obtained from GenBank (http://www.ncbi.nlm.nih.gov).

Two isoforms of AQP4 have been identified: a long isoform (323 amino acids) and a shorter one (301 amino acids). For the purpose of sequence coverage, we studied the longer isoform. While reports indicate that the short form outnumbers the long form by at least 3:1 (56), both protein isoforms are expressed in brain, and the shorter isoform is primarily found in other tissues and may thus be relevant to phenotypes other than cerebral edema (27). Primers were designed manually to span the exons and include approximately 50 bp of flanking intronic sequence. To identify variants of *AQP4*, all five exons and flanking sequences were sequenced. Polymerase chain reaction and sequencing were carried out as previously described. We previously estimated a 5% false positive rate for identifying polymorphisms and a false negative rate of 9.0×10^{-6} SNPs missed per bp screened. We compared the SNPs we found with those in dbSNP (http://www.ncbi.nlm.nih.gov/entrez/query.fcgi?CMD=search&DB=snp), Ensembl (http://www.ensembl.org) and HapMap (http://www.hapmap.org) to determine which were novel. We used Haploview (http://www.broad.mit.edu/mpg/haploview/) to assess haplotype and linkage data. Variant data are available at http://www.PharmGKB.org. This study was approved by UCSF's Committee on Human Research.

Computational prediction

We used four software servers or substitution matrices as well as qualitative analysis to predict the effects of the four nsSNPs we found and the previously documented nsSNP. Of the servers, SIFT (http://blocks.fhcrc.org/sift/SIFT.html) assesses sequence conservation, and MUpro (http://www.ics.uci.edu/~baldig/mutation.html) assesses protein stability. The substitution matrices, PAM40 and Blosum62, are based on evolutionary conservation. We also performed exploratory sequence and structure analysis. For example, we queried NCBI's Entrez Gene (http://www.ncbi.nlm.nih.gov/entrez/

query.fcgi?CMD=search&DB=gene) to identify *AQP4* orthologs and paralogs and constructed multiple sequence alignments for each set using ClustalW (http://www.ebi.ac.uk/clustalw/). We also examined the experimentally determined rat AQP4 structure (code 2d57, Protein Data Bank, www.pdb.org) (Fig. 1C) using the UCSF Chimera molecular visualization software (57).

Mutagenesis and cell culture

The *AQP4* (RefSeq NM_001650.4) coding sequence from IMAGE clone 4717755 was subcloned into the expression vector pcDNA5/FRT (Invitrogen). Clones for all non-synonymous *AQP4* variants were constructed by site-directed mutagenesis of the reference sequence using the QuikChange mutagenesis protocol (Stratagene). The complete coding regions of all variants were sequenced to ensure that the appropriate nucleotide change had occurred and to confirm that no other alterations had been introduced. Chinese Hamster Ovary (CHO) cell lines stably expressing AQP4 or one of its variants were created using the Flp-In system and the corresponding Flp-In-CHO cell line as per the manufacturer's protocol (Invitrogen). Since the Flp-In system utilizes a site-specific recombinase, all AQP4 variants are integrated into the genome at the same locus, the site of a specific sequence engineered into the Flp-In-CHO cell line.

Cell-surface biotinylation

Cell-surface biotinylation was used to quantify the functional pool of AQP4 protein trafficked into the cell membrane. Cell cultures were grown to confluency in T75 flasks and incubated in ice-cold saline solution containing 0.5 mg/ml Sulfo-NHS-Biotin (Pierce) at 4°C for 30 min. Cultures were washed two times in saline and excess biotin was quenched with 3% BSA followed by another set of rinsing. Cells were then removed from the flasks, lysed in buffer containing 0.1% SDS in PBS, 20 μg/ml PMSF. The cell lysate was spun at 10 000 g and the supernatant was collected. Following protein concentration measurement (BCA™ Protein Assay Reagent, Pierce), a 5 μg protein aliquot was kept for loading control, and 50 μg of protein was incubated with a 100 μl slurry of streptavidin beads (Pierce) overnight at 4°C to isolate the membrane proteins. Centrifuging at 10 000 g for 1 min pulled down biotin-streptavidin complexes and following extensive washes, the bound protein was eluted in Lamely buffer at 37°C.

Western blot

Although the Flp-In system gives a high probability of a single copy of the transfected plasmid, aliquots of the cells were saved to assess AQP4 protein expression. Cells were homogenized in buffer containing 250 mM sucrose in PBS and 20 μg/μl PMSF. Homogenate was centrifuged at 15 000 g and after careful assessment of the protein-signal correlation, 6 μg of supernatant was loaded onto 10–12% polyacrylamide gels (Invitrogen). Protein was transferred overnight at 15 V at 4°C onto PVDF membranes (Amersham). After 1 h blocking with 3% skimmed milk (Bio-Rad), blots were probed with primary antibody against AQP4 (Chemicon) for 1 h at a dilution of 1:1000 in 1% BSA. Following extensive washes in Tris-Buffered Saline Tween, blots were incubated with horseradish peroxidase conjugated secondary antibody (1:5000) and detected with electrochemiluminescence (ECL) kit (Amersham). To confirm the specificity of membrane protein detection, blots were stripped according to the manufacturer's instructions and re-probed for the intracellular housekeeping protein glyceraldehyde-phosphate dehydrogenase (GAPDH) with a 1:2000 dilution of monoclonal antibody from Chemicon. This was followed by extensive washes and detection using anti-mouse peroxidase conjugated antibody. Densitometry of the protein bands were assessed with ImageJ, and AQP4 expression was normalized to GAPDH expression.

Water permeability measurements

We assessed osmotic water permeability (P_f), in cells with the well-established method of stopped-flow light scattering (22) using a Hi-Tech Sf-51 instrument. Cells were exposed to hypo- or hyper-tonic solution, and cell swelling or shrinking was measured by a change in diffraction of light. For light scatter measurements, a cell-covered coverslip was sealed at the bottom of an aluminum perfusion chamber (volume 80 ml). A plain coverslip served as the top cover. The chamber was held in a brass thermostatic collar maintained at 37°C and placed on the stage of an inverted microscope (Nikon Diaphot 200). The solutions were perfused via gravity flow in excess of 4–6 chamber volumes/min. Light from a halogen lamp (20 W) was filtered (>420 nm) and focused onto the cells through an achromatic lens from above the stage at an adjustable angle of incidence. In most experiments, the beam subtended at 40° to the plane of the coverslip and had a spot size of approximately 1 mm. Light scattered in the forward direction was collected by a long-working distance objective (Olympus PL2; 20; working distance 1.2 cm; NA = 0.4) with a field of view of approximately 600–800 cells. The scattered light intensity was then directed to a photomultiplier tube (HC125-01, Hamamatsu) by a dichroic mirror centered at 520 nm. Suspensions of cells in PBS were subjected to a 250 mM inwardly directed gradient of sucrose. The water permeability kinetics of increasing cell volume was assessed from the time course of 90° scattered light intensity at 530 nm wavelength. Osmotic water permeability coefficients were calculated from the $t_{1/2}$ of the exponential curve fitted to the time course light scattering as previously described (23). Relative P_f was deduced from the $t_{1/2}$ values normalized to AQP4 membrane protein expression. Three different passages of cells were used for relative water permeability measurements and at least five curves of each cell line were analyzed. Results are reported as mean ± SEM, and significance was assessed by Student's *t*-test at a level of $P = 0.05$.

ACKNOWLEDGEMENTS

We thank Alan Verkman for helpful discussions, Melanie de la Cruz in the UCSF Genome Core Facility for assistance

with *AQP4* sequencing and Doug Stryke and Michiko Kawamoto in the PMT Bioinformatics Core.

Conflict of Interest statement. None declared.

FUNDING

Supported by NIH grants NS049691 (MDS) and NS050173 (GTM), and the UCSF Brain and Spinal Injury Center.

REFERENCES

1. Manley, G.T., Fujimura, M., Ma, T., Noshita, N., Filiz, F., Bollen, A.W., Chan, P. and Verkman, A.S. (2000) Aquaporin-4 deletion in mice reduces brain edema after acute water intoxication and ischemic stroke. *Nat. Med.*, **6**, 159–163.
2. Hiroaki, Y., Tani, K., Kamegawa, A., Gyobu, N., Nishikawa, K., Suzuki, H., Walz, T., Sasaki, S., Mitsuoka, K., Kimura, K., Mizoguchi, A. and Fujiyoshi, Y. (2006) Implications of the aquaporin-4 structure on array formation and cell adhesion. *J. Mol. Biol.*, **355**, 628–639.
3. Jung, J.S., Preston, G.M., Smith, B.L., Guggino, W.B. and Agre, P. (1994) Molecular structure of the water channel through aquaporin CHIP. The hourglass model. *J. Biol. Chem.*, **269**, 14648–14654.
4. Walz, T., Hirai, T., Murata, K., Heymann, J.B. and Mitsuoka, K. (1997) The three-dimensional structure of aquaporin-1. *Nature*, **387**, 624–627.
5. Jung, J.S., Bhat, R.V., Preston, G.M., Guggino, W.B., Baraban, J.M. and Agre, P. (1994) Molecular characterization of an aquaporin cDNA from brain: candidate osmoreceptor and regulator of water balance. *Proc. Natl Acad. Sci. USA*, **91**, 13052–13056.
6. Zelenina, M., Bondar, A.A., Zelenin, S. and Aperia, A. (2003) Nickel and extracellular acidification inhibit the water permeability of human aquaporin-3 in lung epithelial cells. *J. Biol. Chem.*, **278**, 30037–30043.
7. Beitz, E., Zenner, H.P. and Schultz, J.E. (2003) Aquaporin-mediated fluid regulation in the inner ear. *Cell. Mol. Neurobiol.*, **23**, 315–329.
8. Deen, P.M., Croes, H., van Aubel, R.A., Ginsel, L.A. and van Os, C.H. (1995) Water channels encoded by mutant aquaporin-2 genes in nephrogenic diabetes insipidus are impaired in their cellular routing. *J. Clin. Invest.*, **95**, 2291–2296.
9. Marr, N., Bichet, D.G., Lonergan, M., Arthus, M.F., Jeck, N., Seyberth, H.W., Rosenthal, W., van Os, C.H., Oksche, A. and Deen, P.M. (2002) Heteroligomerization of an Aquaporin-2 mutant with wild-type Aquaporin-2 and their misrouting to late endosomes/lysosomes explains dominant nephrogenic diabetes insipidus. *Hum. Mol. Genet.*, **11**, 779–789.
10. de Mattia, F., Savelkoul, P.J., Kamsteeg, E.J., Konings, I.B., van der Sluijs, P., Mallmann, R., Oksche, A. and Deen, P.M. (2005) Lack of arginine vasopressin-induced phosphorylation of aquaporin-2 mutant AQP2-R254L explains dominant nephrogenic diabetes insipidus. *J. Am. Soc. Nephrol.*, **16**, 2872–2880.
11. Canfield, M.C., Tamarappoo, B.K., Moses, A.M., Verkman, A.S. and Holtzman, E.J. (1997) Identification and characterization of aquaporin-2 water channel mutations causing nephrogenic diabetes insipidus with partial vasopressin response. *Hum. Mol. Genet.*, **6**, 1865–1871.
12. Shi, L.B. and Verkman, A.S. (1996) Selected cysteine point mutations confer mercurial sensitivity to the mercurial-insensitive water channel MIWC/AQP-4. *Biochemistry*, **35**, 538–544.
13. Nebert, D.W. (2002) Proposal for an allele nomenclature system based on the evolutionary divergence of haplotypes. *Hum. Mutat.*, **20**, 463–472.
14. Lewontin, R.C. (1964) The Interaction of Selection and Linkage. I. General considerations; heterotic models. *Genetics*, **49**, 49–67.
15. Balding, D.J. (2006) A tutorial on statistical methods for population association studies. *Nat. Rev. Genet.*, **10**, 781–791.
16. Dayhoff, M.O. (1979) *Atlas of Protein Sequences and Structure*. National Biomedical Research Foundation, Washington, DC, USA, Vol. 5, Suppl. 3, pp. 353–358.
17. Henikoff, S. and Henikoff, J.G. (1993) Performance evaluation of amino acid substitution matrices. *Proteins*, **17**, 49–61.
18. Ng, P.C. and Henikoff, S. (2001) Predicting deleterious amino acid substitutions. *Genome Res.*, **11**, 863–874.
19. Cheng, J., Randall, A. and Baldi, P. (2006) Prediction of protein stability changes for single-site mutations using support vector machines. *Proteins*, **62**, 1125–1132.
20. Neely, J.D., Amiry-Moghaddam, M., Ottersen, O.P., Froehner, S.C., Agre, P. and Adams, M.E. (2001) Syntrophin-dependent expression and localization of Aquaporin-4 water channel protein. *Proc. Natl Acad. Sci. USA*, **98**, 14108–14113.
21. Verkman, A.S., Weyer, P., Brown, D. and Ausiello, D.A. (1989) Functional water channels are present in clathrin-coated vesicles from bovine kidney but not from brain. *J. Biol. Chem.*, **264**, 20608–20613.
22. van Hoek, A.N. and Verkman, A.S. (1992) *J. Biol. Chem.*, **267**, 18267–18269.
23. Verkman, A.S. (2000) Water permeability measurement in living cells and complex tissues. *J. Membr. Biol.*, **173**, 73–87.
24. Yang, B. and Verkman, A.S. (1997) Water and glycerol permeabilities of aquaporins 1-5 and MIP determined quantitatively by expression of epitope-tagged constructs in Xenopus oocytes. *J. Biol. Chem.*, **272**, 16140–16146.
25. Mhatre, A.N., Stern, R.E., Li, J. and Lalwani, A.K. (2002) Aquaporin 4 expression in the mammalian inner ear and its role in hearing. *Biochem. Biophys. Res. Commun.*, **297**, 987–996.
26. Castellanos, M., Perez de la Ossa, N., Moldes, O., Lizasoain, I., Serena, J., Rodriguez, R., Sobrino, T., Vivancos, J., Silva, Y. and Mallolas, J. (2007) A polymorphism in the 5′ untranslated region of the Aquaporin 4 gene is related to parenchymal hemorrhage in patients with acute ischemic stroke. European Stroke Conference, Glasgow, UK.
27. Umenishi, F. and Verkman, A.S. (1998) Isolation and functional analysis of alternative promoters in the human aquaporin-4 water channel gene. *Genomics*, **50**, 373–377.
28. Wellcome Trust Case Control Consortium. (2007) Genome-wide association study of 14,000 cases of seven common diseases and 3,000 shared controls. *Nature*, **7145**, 661–678.
29. Verkman, A.S., Binder, D.K., Bloch, O., Auguste, K. and Papadopoulos, M.C. (2006) Three distinct roles of aquaporin-4 in brain function revealed by knockout mice. *Biochim. Biophys. Acta*, **1758**, 1085–1093.
30. Nicchia, G.P., Srinivas, M., Li, W., Brosnan, C.F., Frigeri, A. and Spray, D.C. (2005) New possible roles for aquaporin-4 in astrocytes: cell cytoskeleton and functional relationship with connexin43. *FASEB J.*, **19**, 1674–1676.
31. Urban, T.J., Sebro, R., Hurowitz, E.H., Leabman, M.K., Badagnani, I., Lagpacan, L.L., Risch, N. and Giacomini, K.M. (2006) Functional genomics of membrane transporters in human populations. *Genome Res.*, **16**, 223–230.
32. Wang, Z. and Moult, J. (2001) SNPs, protein structure, and disease. *Hum. Mutat.*, **17**, 263–270.
33. Nagelhus, E.A., Mathiisen, T.M. and Ottersen, O.P. (2004) Aquaporin-4 in the central nervous system: cellular and subcellular distribution and coexpression with KIR4.1. *Neuroscience*, **129**, 905–913.
34. Berry, V., Francis, P., Kaushal, S., Moore, A. and Bhattacharya, S. (2000) Missense mutations in MIP underlie autosomal dominant 'polymorphic' and lamellar cataracts linked to 12q. *Nat Genet.*, **25**, 15–17.
35. Preston, G.M., Jung, J.S., Guggino, W.B. and Agre, P. (1993) The mercury-sensitive residue at cysteine 189 in the CHIP28 water channel. *J. Biol. Chem.*, **268**, 17–20.
36. Hochberg, Z., Van Lieburg, A., Even, L., Brenner, B., Lanir, N., Van Oost, B.A. and Knoers, N.V. (1997) Autosomal recessive nephrogenic diabetes insipidus caused by an aquaporin-2 mutation. *J. Clin. Endocrinol. Metab.*, **82**, 686–689.
37. Lin, S.H., Bichet, D.G., Sasaki, S., Kuwahara, M., Arthus, M.F., Lonergan, M. and Lin, Y.F. (2002) Two novel aquaporin-2 mutations responsible for congenital nephrogenic diabetes insipidus in Chinese families. *J. Clin. Endocrinol. Metab.*, **87**, 2694–2700.
38. Carroll, P., Al-Mojalli, H., Al-Abbad, A., Al-Hassoun, I., Al-Hamed, M., Al-Amr, R., Butt, A.I. and Meyer, B.F. (2006) Novel mutations underlying nephrogenic diabetes insipidus in Arab families. *Genet. Med.*, **8**, 443–447.
39. Zelenina, M., Zelenin, S., Bondar, A.A., Brismar, H. and Aperia, A. (2002) Water permeability of aquaporin-4 is decreased by protein kinase C and dopamine. *Am. J. Physiol. Renal Physiol.*, **283**, F309–F318.
40. Okamura, T., Miyoshi, I., Takahashi, K., Mototani, Y., Ishigaki, S., Kon, Y. and Kasai, N. (2003) Bilateral congenital cataracts result from a gain-of-function mutation in the gene for aquaporin-0 in mice. *Genomics*, **81**, 361–368.

41. Sidjanin, D.J., Parker-Wilson, D.M., Neuhauser-Klaus, A., Pretsch, W., Favor, J., Deen, P.M., Ohtaka-Maruyama, C., Lu, Y., Bragin, A., Skach, W.R. *et al.* (2001) A 76-bp deletion in the Mip gene causes autosomal dominant cataract in Hfi mice. *Genomics*, **74**, 313–319.
42. Madrid, R., Le Maout, S., Barrault, M.B., Janvier, K., Benichou, S. and Merot, J. (2001) Polarized trafficking and surface expression of the AQP4 water channel are coordinated by serial and regulated interactions with different clathrin-adaptor complexes. *EMBO J.*, **24**, 7008–7021.
43. Nakahama, K., Fujioka, A., Nagano, M., Satoh, S., Furukawa, K., Sasaki, H. and Shigeyoshi, Y. (2002) A role of the C-terminus of aquaporin 4 in its membrane expression in cultured astrocytes. *Genes Cells*, **7**, 731–741.
44. Xiang, H., Tschirret-Guth, R.A. and Ortiz De Montellano, P.R. (2000) An A245T mutation conveys on cytochrome P450eryF the ability to oxidize alternative substrates. *J. Biol. Chem.*, **275**, 35999–36006.
45. Zuo, J., De Jager, P.L., Takahashi, K.A., Jiang, W., Linden, D.J. and Heintz, N. (1997) Neurodegeneration in Lurcher mice caused by mutation in delta2 glutamate receptor gene. *Nature*, **388**, 769–773.
46. Saadoun, S., Papadopoulos, M.C., Watanabe, H., Yan, D., Manley, G.T. and Verkman, A.S. (2005) Involvement of aquaporin-4 in astroglial cell migration and glial scar formation. *J. Cell. Sci.*, **118**, 5691–5698.
47. Binder, D.K., Oshio, K., Ma, T., Verkman, A.S. and Manley, G.T. (2004) Increased seizure threshold in mice lacking aquaporin-4 water channels. *Neuroreport*, **15**, 259–262.
48. Lee, T.S., Eid, T., Mane, S., Kim, J.H., Spencer, D.D., Ottersen, O.P. and de Lanerolle, N.C. (2004) Aquaporin-4 is increased in the sclerotic hippocampus in human temporal lobe epilepsy. *Acta Neuropathol. (Berl.)*, **108**, 493–502.
49. Wakayama, Y., Jimi, T., Inoue, M., Kojima, H., Murahashi, M., Kumagai, T., Yamashita, S., Hara, H. and Shibuya, S. (2002) Reduced aquaporin 4 expression in the muscle plasma membrane of patients with Duchenne muscular dystrophy. *Arch. Neurol.*, **59**, 431–437.
50. St.Hillaire, C., Vargas, D., Pardo, C.A., Gincel, D., Mann, J., Rothstein, J.D., McArthur, J.C. and Conant, K. (2005) Aquaporin 4 is increased in association with human immunodeficiency virus dementia: implications for disease pathogenesis. *J. Neurovirol.*, **11**, 535–543.
51. Alexander, J.J., Bao, L., Jacob, A., Kraus, D.M., Holers, V.M. and Quigg, R.J. (2003) Administration of the soluble complement inhibitor, Crry-Ig, reduces inflammation and aquaporin 4 expression in lupus cerebritis. *Biochim. Biophys. Acta*, **1639**, 169–176.
52. Sinclair, C., Kirk, J., Herron, B., Fitzgerald, U. and McQuaid, S. (2007) Absence of aquaporin-4 expression in lesions of neuromyelitis optica but increased expression in multiple sclerosis lesions and normal-appearing white matter. *Acta Neuropathol. (Berl.)*, **113**, 187–194.
53. Hardin, J.A., Wallace, L.E., Wong, J.F., O'Loughlin, E.V., Urbanski, S.J., Gall, D.G., MacNaughton, W.K. and Beck, P.L. (2004) Aquaporin expression is downregulated in a murine model of colitis and in patients with ulcerative colitis, Crohn's disease and infectious colitis. *Cell Tissue Res.*, **318**, 313–323.
54. Fan, Y., Kong, H., Shi, X., Sun, X., Ding, J., Wu, J. and Hu, G. (2007) Hypersensitivity of aquaporin 4-deficient mice to 1-methyl-4-phenyl-1,2,3,6-tetrahydropyrindine and astrocytic modulation. *Neurobiol. Aging*, in press.
55. Leabman, M.K., Huang, C.C., DeYoung, J., Carlson, E.J., Taylor, T.R., de la Cruz, M., Johns, S.J., Stryke, D., Kawamoto, M., Urban, T.J. *et al.* Pharmacogenetics Of Membrane Transporters Investigators. (2003) Natural variation in human membrane transporter genes reveals evolutionary and functional constraints. *Proc. Natl Acad. Sci. USA*, **100**, 5896–5901.
56. Neely, J.D. and Christensen, B.M. (1999) Heterotetrameric composition of aquaporin-4 water channels. *Biochemistry*, **38**, 11156–11163.
57. Pettersen, E.F., Goddard, T.D., Huang, C.C., Couch, G.S., Greenblatt, D.M., Meng, E.C. and Ferrin, T.E. (2004) UCSF Chimera—a visualization system for exploratory research and analysis. *J. Comput. Chem.*, **25**, 1605–1612.
58. Yang, B., Verbavatz, J.M., Song, Y., Vetrivel, L., Manley, G., Kao, W.M., Ma, T. and Verkman, A.S. (2000) Skeletal muscle function and water permeability in aquaporin-4 deficient mice. *Am. J. Physiol. Cell Physiol.*, **278**, C1108–C1115.